



# FXR mediates ILC-intrinsic responses to intestinal inflammation

Ting Fu<sup>a</sup>, Yuwenbin Li<sup>a</sup>, Tae Gyu Oh<sup>a</sup> , Fritz Cayabyab<sup>a</sup>, Nanhai He<sup>a</sup>, Qin Tang<sup>a</sup>, Sally Coulter<sup>b</sup>, Morgan Truitt<sup>a</sup>, Paul Medina<sup>a</sup>, Mingxiao He<sup>a</sup>, Ruth T. Yu<sup>a</sup> , Annette Atkins<sup>a</sup> , Ye Zheng<sup>c</sup>, Christopher Liddle<sup>b</sup> , Michael Downes<sup>a,1</sup> , and Ronald M. Evans<sup>a,1</sup>

Contributed by Ronald M. Evans; received July 29, 2022; accepted November 10, 2022; reviewed by David D. Moore and Enrique Saez

The pleiotropic actions of the Farnesoid X Receptor (FXR) are required for gut health, and reciprocally, reduced intestinal FXR signaling is seen in inflammatory bowel diseases (IBDs). Here, we show that activation of FXR selectively in the intestine is protective in inflammation-driven models of IBD. Prophylactic activation of FXR restored homeostatic levels of pro-inflammatory cytokines, most notably IL17. Importantly, these changes were attributed to FXR regulation of innate lymphoid cells (ILCs), with both the inflammation-driven increases in ILCs, and ILC3s in particular, and the induction of *Il17a* and *Il17f* in ILC3s blocked by FXR activation. Moreover, a population of ILC precursor-like cells increased with treatment, implicating FXR in the maturation/differentiation of ILC precursors. These findings identify FXR as an intrinsic regulator of intestinal ILCs and a potential therapeutic target in inflammatory intestinal diseases.

inflammatory bowel disease | bile acids | FXR | innate lymphoid cells | IL17

Inflammatory bowel disease (IBD) is a chronic intestinal disorder that affects 4 million individuals worldwide. While the underlying cause(s) is not fully understood, defective epithelial barrier function and aberrant intestinal immune responses contribute to the inflammatory responses that drive the chronic disease. Loss of epithelial tight junctions exposes innate immune cells to commensal microbiota to induce cytokines that subsequently initiate an inflammatory response in adaptive immune cells (1–3). Thus, a complex interplay between epithelial cells, the innate and adaptive immune systems, and the microbiome contributes to the pathogenesis of IBD (2–5).

Innate lymphoid cells (ILCs) characteristically express the IL-7 receptor and are found in mucosal tissues including that in the intestine (6, 7). ILCs are subtyped into 3 major groups based on signature transcription factor expression and cytokine secretion, analogous to helper T cell grouping (8). Unique tissue-specific ILC repertoires have been attributed to the differentiation of circulating precursors in response to local environmental cues (9). Within the intestine, ILCs are important for intestinal barrier function and innate immunity, where integration of microbial signals generates phenotypic and functional plasticity (8–11). Consistent with the notion of cellular plasticity, recent single-cell studies identified multiple discrete ILC subsets in human ileal lamina propria (LP), including cells coexpressing markers of ILC3s and ILC1s (12). Notably, an increase in the number of actively proliferating ILCs was seen in the LP of Crohn's disease patients (2, 10, 11, 13–16).

Consistent with a role in maintaining intestinal homeostasis, the development of precursor ILCs can be influenced by nutritional cues that tailor the frequencies of ILC subtypes to specific intestinal challenges, thereby directly coupling the intestinal innate immune response with diet (11). Similarly, the adaptive immune system has been shown to be responsive to dietary-related signals, whereby intestinal T cell homeostasis is dependent on the ability of T<sub>eff</sub> cells to appropriately respond to bile acids (BAs) (17). BAs are cholesterol-based metabolites that regulate mucosal homeostasis and inflammation. Secreted into the duodenum to facilitate the absorption of dietary lipids and fat-soluble vitamins, they are subsequently reabsorbed in the ileum where they accumulate in the LP prior to transiting to the portal circulation. In addition to solubilizing fats, BAs function as key signaling molecules involved in the regulation of metabolic processes. Indeed, BA homeostasis is tightly controlled by the transcriptional activities of the farnesoid x receptor (FXR) (18), and loss of BA homeostasis has been implicated in the pathogenesis of IBD. We have evolved gut-selective small-molecule FXR agonists (fexaramine (Fex) and FexD) (19) and shown that Fex treatment results in dramatic metabolic improvements in obesity and related metabolic diseases (20).

Cellular crosstalk between the epithelium and the intestinal immune system is critical in maintaining gut integrity and protecting against pathogen-initiated inflammation (1, 3). Increased intestinal levels of the cytokines IL17 and IL23 have been causally associated with IBD (21–23). While IL17A is implicated in the maintenance of intestinal tight junctions, IL17F is associated with intestinal damage, and antibodies to IL17F are

## Significance

In addition to promoting lipid and fat-soluble vitamin absorption, bile acids (BAs) function as signaling molecules that coordinate persistent changes in intestinal cells. As such, BA homeostasis is tightly regulated by the Farnesoid X Receptor (FXR). This study elucidates a previously unknown role for FXR in regulating innate lymphoid cells (ILCs), wherein activation of FXR abrogates ILC3-dependent intestinal inflammation. Establishing FXR as an intrinsic regulator of ILCs provides a functional connection between diet and innate immunity. Moreover, with synergistic effects in both intestinal epithelial and immune cells, these findings implicate FXR agonism as an integrative therapeutic strategy for chronic intestinal inflammation.

Author contributions: T.F., R.T.Y., A.A., M.D., and R.M.E. designed research; T.F., Y.L., F.C., N.H., Q.T., and M.H. performed research; T.F., Y.L., T.G.O., F.C., N.H., Q.T., S.C., M.T., P.M., R.T.Y., Y.Z., and C.L. analyzed data; Q.T. and P.M. technical assistance; M.T. and Y.Z. scientific input; M.H. mouse maintenance; R.T.Y. and R.M.E. supervised the research; A.A. and M.D. supervised research; and T.F., R.T.Y., A.A., M.D., and R.M.E. wrote the paper.

Reviewers: D.D.M., University of California Berkeley; and E.S., The Scripps Research Institute.

Competing interest statement: The authors declare a competing interest. The authors have patent filings to disclose, we have an issued patent related to fexaramine.

Copyright © 2022 the Author(s). Published by PNAS. This article is distributed under Creative Commons Attribution-NonCommercial-NoDerivatives License 4.0 (CC BY-NC-ND).

<sup>1</sup>To whom correspondence may be addressed. Email: evans@salk.edu and downes@salk.edu.

This article contains supporting information online at <https://www.pnas.org/lookup/suppl/doi:10.1073/pnas.2213041119/-DCSupplemental>.

Published December 12, 2022.

protective in the mouse model of colitis (24). Th17 and ILC3 cells secrete IL17; however, the relative contributions of specific immune cell types to IBD have not been clearly established (13, 23). Here, we elucidate a previously unknown role for FXR in the regulation of IL17 production in intestinal ILC3s. Moreover, the increase in an ILC precursor-like population seen with FexD treatment implicates FXR in the maturation/differentiation of intestinal ILCs.

## Results

**Inflammation Reshapes the Villi Structure.** The crypt-villi architecture is integral for normal intestinal regeneration and bile acid homeostasis (20, 25–28). Here, we used a dextran sulfate sodium (DSS)-induced model of colitis to explore the consequences of inflammatory damage to the villi structure (29). Acute DSS (ADSS) treatment (5% DSS in drinking water for 5 to 7 d, ADSS) caused profound morphological changes including epithelial erosion, irregular hyperplastic crypt formation, a reduction in villi length, and aberrantly shaped Goblet and Paneth cells in wild-type (WT) mice (*SI Appendix, Fig. S1 A–D*). These changes were associated with reduced expression of intestinal *Fxr* and its target genes (*Fgf15*, *Ibapb*, *Osta*, and *Ostf*) and a ~2-fold increase in intestinal permeability (*SI Appendix, Fig. S1 E and F*) (27, 28). Consistent with reduced ileal FXR signaling, total BA levels were increased ~2.9 fold, with a disproportionate increase in primary BAs (*SI Appendix, Fig. S1 G*). These changes were due, in large part, to pronounced increases in the levels of the primary BAs  $\beta$ -muricholic acid ( $\beta$ MCA), taurocholic acid (T-CA), and cholic acid (CA) and the secondary BAs deoxycholic acid and  $\omega$ -muricholic acid upon ADSS treatment (*SI Appendix, Fig. S1 H*). In addition, the serum levels of the proinflammatory cytokines IL17 and IL6 approximately doubled, in agreement with the marked increases in ileal *Il17a*, *Il6*, *Il22*, and *Il23* expression in response to the ADSS challenge (*SI Appendix, Fig. S1 I and J*) (5). As expected with epithelial damage, expression of intestinal stem cell (ISC) (30) signature genes *Lgr5* and *Olfm4* was upregulated (*SI Appendix, Fig. S1 J*) (25). The concurrent increase in the stem cell IL17 receptor *Il17rd* raised the possibility that ISC proliferation may be driven by IL17. In support of this notion, IL17 but not IL6, stimulated the growth of intestinal organoids as measured by ATP release and stem cell marker gene expression (*SI Appendix, Fig. S1 K and L*).

**FXR Protects against ADSS-Induced Inflammation.** To explore a causal association between reduced ileal FXR signaling and epithelial dysregulation, we utilized the intestinally restricted FXR agonist, FexD (19, 20, 25). Prophylactic treatment of WT mice with FexD (50 mg/kg/day p.o. for 4 wk prior to the ADSS challenge) was protective against DSS-induced damage, with improvements in intestinal morphology and body weight (Fig. 1 *A* and *B* and *SI Appendix, Fig. S2 A*). Notably, ileal FXR signaling was largely maintained in FexD-treated mice (Fig. 1 *C*). The DSS-induced increase in total serum BAs and the associated compositional changes were partially prevented by FexD treatment; a possible consequence of the severity of the ADSS model (Fig. 1 *D* and *SI Appendix, Fig. S2 B*). In addition, FexD treatment prevented DSS-induced increases in intestinal permeability and reduced the systemic inflammatory response as indicated by spleen size and serum IL17 and IL6 levels (Fig. 1 *E* and *SI Appendix, Fig. S2 C–F*). The reduction in proinflammatory cytokines including *Il17* and IL17-induced genes in immune cells enriched from intestinal LP led to speculation that in addition to its established role in epithelial cells, FXR signaling directly affected immune

cell populations (*SI Appendix, Fig. S2 G*) (17, 26). Notably, in an adoptive T cell transfer model of colitis, FexD-treated mice displayed a less inflammatory phenotype including reduced weight loss and reduced expression of key inflammatory cytokines (*SI Appendix, Fig. S2 H–N*).

To support a role for FXR in immune cells, the FXR-induced changes in immune cell populations were determined. Prophylactic FexD treatment largely blocked the ADSS-induced increases in IL17A<sup>+</sup> and IFN $\gamma$ <sup>+</sup> CD4<sup>+</sup> T cells in ileal LP, with minimal effects on splenic and mesenteric lymph node (MLN) cells (Fig. 1 *F* and *SI Appendix, Fig. S3 A–E*). In addition, the disproportionate increase in ILCs (~10 to 18% of total immune cells in DSS-treated mice) was abrogated by FexD treatment (Fig. 1 *G* and *SI Appendix, Fig. S3 F*). In particular, DSS-induced increases in CCR6<sup>+</sup> and CD4<sup>+</sup> ILC3s and the ~2-fold increase in IL17A<sup>+</sup> and IL17F<sup>+</sup> ILC3s were prevented by FexD treatment (Fig. 1 *G* and *SI Appendix, Fig. S4 A–E*). These findings indicate that activation of FXR was sufficient to restore T cell and ILC homeostatic levels in this intestinal inflammation model.

To support this notion, mice deficient in T cells and ILCs (NSG mice) were prophylactically treated with FexD prior to ADSS (Fig. 1 *H*). The activation of FXR target genes in the intestinal epithelium led to reduced morphological changes; an effect attributed in part to a reduction in fibrotic gene expression (Figs. 1 *I–J* and *SI Appendix, Fig. S5 A–C*). In contrast, while the inflammatory response to ADSS was markedly reduced in NSG mice, FexD treatment failed to restore intestinal BA homeostasis and gut integrity and did not attenuate inflammatory damage (Fig. 1 *K–N* and *SI Appendix, Fig. S5 D–F*). These findings reveal that the beneficial histological effects of FXR activation in the epithelium are separable from the antiinflammatory response in this ADSS model.

**FXR Affects Innate and Adaptive Immunity via ILCs.** To explore the mechanism underlying how FXR modulates the function of immune cells in the ADSS model, we initially determined the functional consequences of FXR signaling in T cells. Naive splenic T cells were differentiated in vitro into Th1, Th2, Th17, and iTreg cells prior to exposure to the synthetic FXR agonist FexD or the natural antagonistic BA tauro- $\beta$ -muricholic acid (T- $\beta$ MCA) (*SI Appendix, Fig. S6 A*). Somewhat unexpectedly, neither activation nor inhibition of FXR signaling affected signature functional markers in Th17, Th1, Th2, or iTregs (*SI Appendix, Fig. S6 B–D*). Treatment with additional synthetic FXR agonists and antagonists, as well as endogenous BA ligands, largely replicated these findings and was consistent with the lack of *Fxr* expression in these cell populations. As in vitro differentiated T cells may not fully recapitulate the activities of in vivo activated T cells, similar experiments were performed with total immune cell populations isolated from both the spleen and MLNs of ADSS-treated mice (*SI Appendix, Fig. S6 E*). Immune cells were cultured ex vivo prior to treatment with either the FXR agonist FexD or the antagonist T- $\beta$ MCA. Subsequent gene expression profiling established that these ex vivo activated cell populations were also largely refractory to FXR ligands (*SI Appendix, Fig. S6 F*). These findings, in combination with essentially undetectable *Fxr* levels, excluded a direct effect of FexD in T cells in attenuating the ADSS-induced phenotype.

Next, the ex vivo responses of immune cells isolated from the small intestinal LP of ADSS-challenged mice were determined. IL17A<sup>+</sup> T cell numbers were not altered by ex vivo FexD treatment (*SI Appendix, Fig. S6 G*), in agreement with the findings with splenic and MLN T cells. In contrast, a marked reduction in the proportion of ILC3s including the percentage of IL17A<sup>+</sup> ILC3s and decreased IL22 secretion were seen with ex vivo FexD treatment (*SI Appendix, Fig. S6 H–K*). This sensitivity of ILCs to FXR

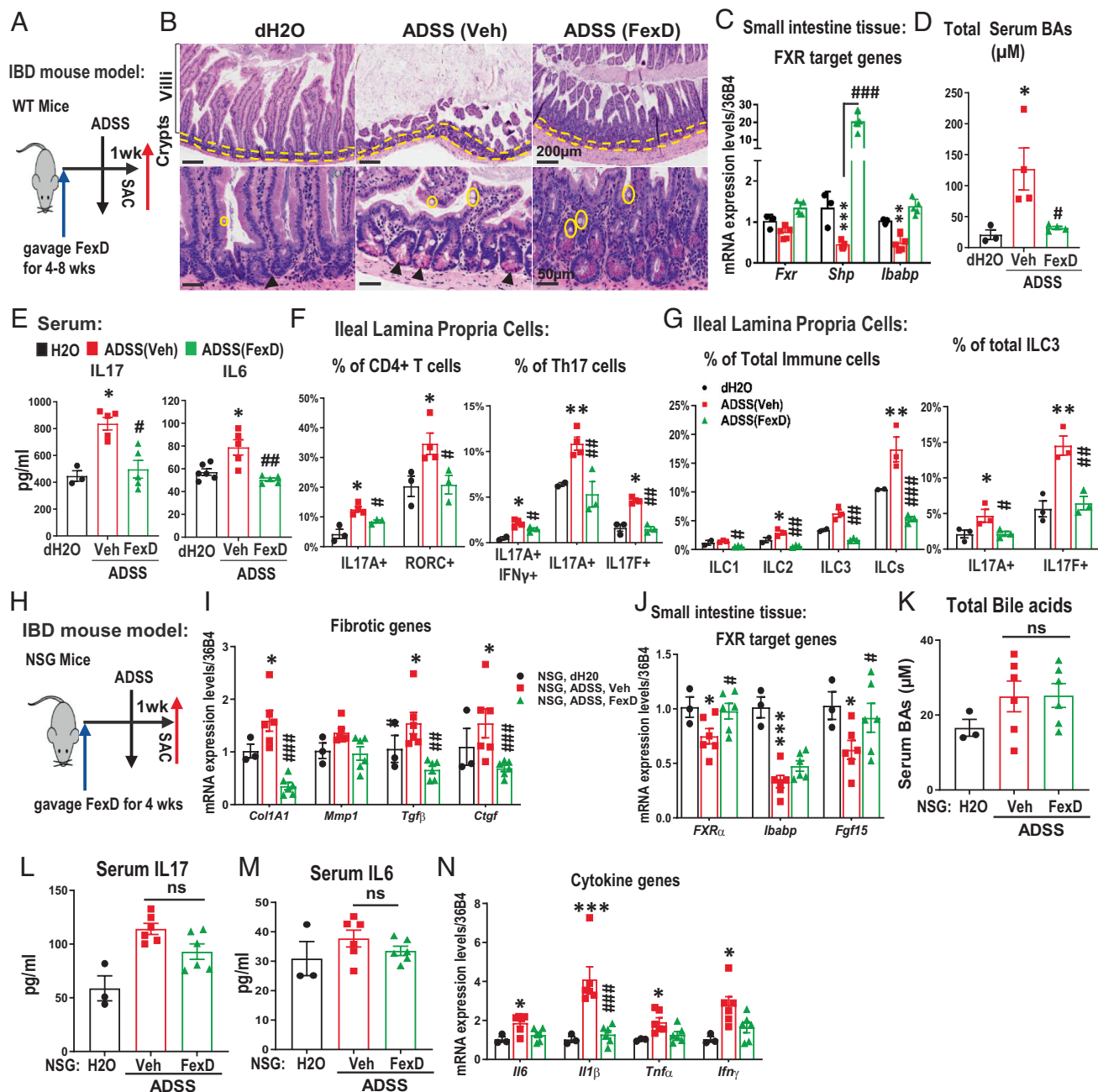


**Fig. 1.** FXR protects against ADSS-induced inflammation. (A) Schematic of ADSS (ADSS, 5% DSS in drinking water) regimen in WT mice treated with vehicle or FexD (50 mg/kg/day p.o.). H<sub>2</sub>O, n = 3; DSS, n = 5; DSS + FexD, n = 5. (B) Representative H&E staining of small intestine. Yellow lines delineate villi and crypt structures, and goblet (yellow circles) and crypt Paneth (arrowheads) cells are indicated. (Scale bars, 200 μm (Upper) and 50 μm (Lower).) (C) Ileal expression of *Fxr* and FXR target genes (n = 5). (D and E) Total serum bile acid (BA) levels (n = 3 to 4) (D) and serum IL17 and IL6 levels (n = 5) levels in 18-wk-old ADSS mouse models (E). (F) Total (Left) and cytokine positive Th17 cells (Right) in small intestinal tissue (n = 3 to 5). Representative FACS analyses in SI Appendix, Fig. S3E. (G) Total ILC subtype (Left) and cytokine positive ILC3s (Right) in small intestinal tissue (n = 3 to 5). Representative FACS analyses in SI Appendix, Fig. S3F. (H) Experimental scheme (NSG mice treated with H<sub>2</sub>O, n = 3; DSS, n = 6; and DSS + FexD, n = 6). (I) Expression of fibrotic genes in small intestine, measured by qRT-PCR. (J) Expression of FXR target genes in small intestine, measured by qRT-PCR. (K–M) Total bile acid (K) and serum IL17 (L) and IL6 (M) levels. (N) Expression of cytokine genes in small intestine, measured by qRT-PCR. WT mice under ADSS were independently replicated ten times and NSG experiments were independently replicated two times, and representative data in one experiment are shown as the mean ± SEM. \* ADSS versus vehicle; # FexD versus ADSS; \* and # P < 0.05; \*\* and ### P < 0.01; \*\*\* and ### P < 0.005; and ns—not significant. One-way ANOVA test followed by multiple comparisons were used for three group comparisons.

ligands was supported by gene expression profiling, where both FXR target genes and signature cytokine genes including *Il17a*, *Il22*, and *Ifnγ* were responsive to agonist and antagonist treatments (SI Appendix, Fig. S6 L–M).

**FXR Modulates ILC Response to Inflammatory Insult.** The disparity between in vivo and ex vivo effects of FexD on IL17A<sup>+</sup> T cells raised the possibility of ILC/T cell crosstalk (Fig. 1F compared

to SI Appendix, Fig. S6G) (31–33). Indeed, proinflammatory cytokines such as IL6 are known to affect immune cells locally and systemically. To explore possible crosstalk, T and ILC populations from the LP of ADSS-treated mice were sorted prior to treatment with FXR ligands (Fig. 2A). As seen with in vitro differentiated T cells, *Fxr* expression and regulation of FXR target genes were not seen in the isolated T cell population (SI Appendix, Fig. S6N). In contrast, the sorted ILC population had measurable levels of *Fxr*



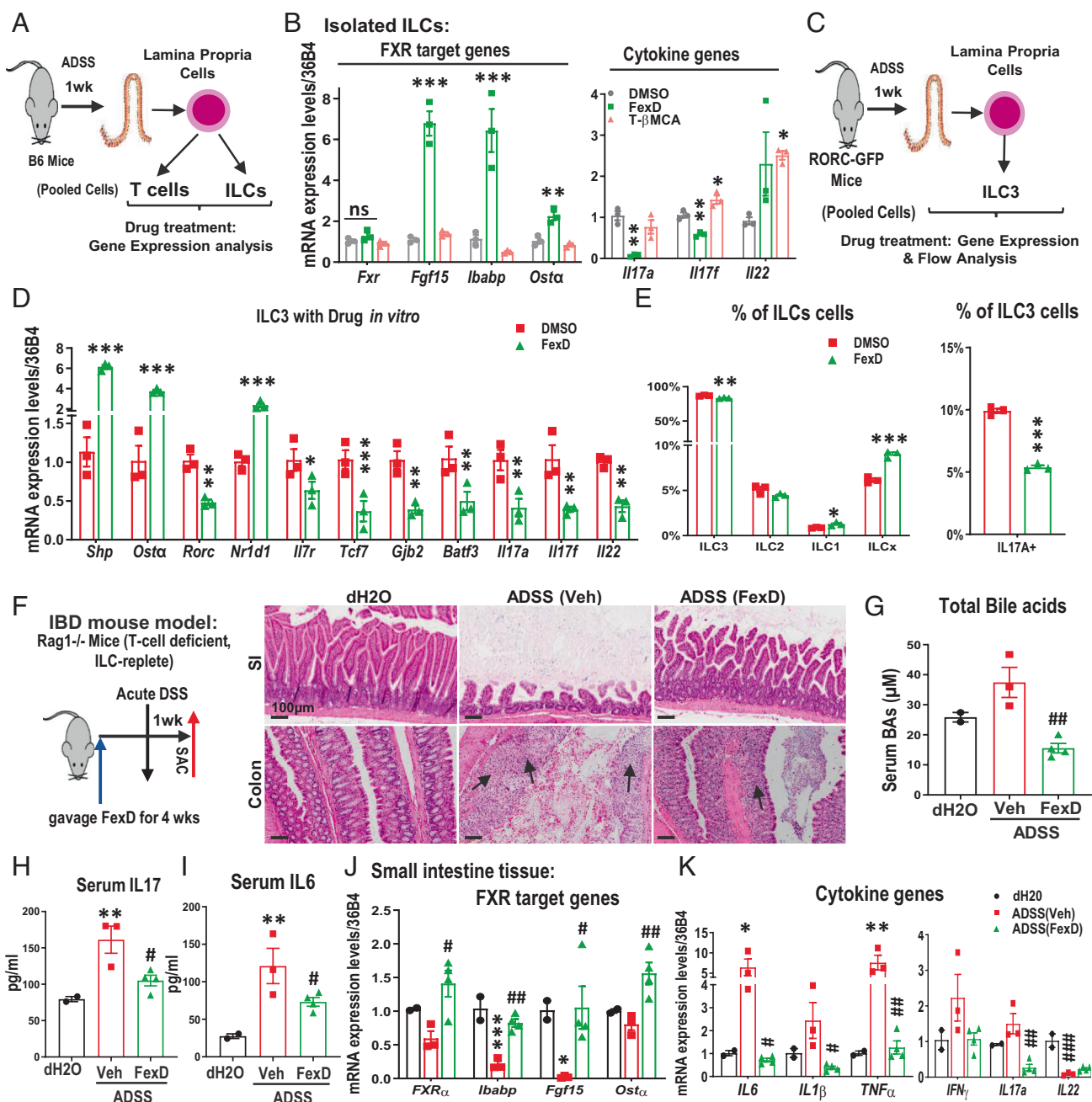


**Fig. 2.** FXR modulates ILC responses to inflammatory insults. (A and B) Experimental scheme (n = 12 pooled) (A), and FXR target and selected cytokine gene expression in isolated ILCs (B) (n = 3). (C and D) Experimental scheme (n = 12 pooled) (C), and gene expression in isolated ILC3s (D). (E) Quantification of ILCs and ILC3 percentages. (F) Experimental scheme and representative H&E staining of small intestine (SI) and colon. Arrows indicate neutrophil infiltration (Scale bar, 100  $\mu$ m.) (G–I) Total serum bile acid (G), IL17 (H), and IL6 levels (I) (n = 3 and 4). (J and K) Expression of FXR target (J) and marker cytokine (K) genes in small intestinal tissue, measured by qRT-PCR. Experiments were independently replicated two times, with representative data shown as the mean  $\pm$  SEM. \* ADSS versus vehicle; # FexD versus ADSS; \*  $p < 0.05$ ; \*\*  $p < 0.01$ ; \*\*\*  $p < 0.005$ ; and ns—not significant. Student's unpaired *t* test was used for two group comparisons; one-way ANOVA test followed by multiple comparisons was used for three-way comparisons.

expression, and FXR target genes including *Fgf15* and *Ibabp* were induced upon FexD treatment (Fig. 2B). Notably, FexD treatment reduced *Il17a* expression only in the ILC population, suggesting that the beneficial effects of FXR activation are mediated by ILCs (Fig. 2B). These findings were recapitulated in ILC3s sorted from *Rorc*-EGFP mice, where ex vivo FexD treatment decreased the expression of identity markers (*Rorc*, *Tcf7*, *Gjb2*, and *Batf3*) and cytokine genes (*Il17a* and *Il17f*) (Fig. 2C and D and SI Appendix, Fig. S7A), implicating FXR in the functional maturation of ILC3s. Moreover, changes in the ILC subtype composition were evident with FexD treatment, including reductions in *IL17A*<sup>+</sup> and *CCR6*<sup>+</sup>

ILC3 subpopulations, suggestive of a developmental role for FXR (Fig. 2E and SI Appendix, Fig. S7A–C).

The above ex vivo findings implicated FXR signaling in ILCs in the protective effects of FexD treatment. To further support this notion, T cell-deficient mice (*Rag1*<sup>−/−</sup> mice) were prophylactically treated with FexD prior to ADSS. In the absence of T cells, FexD treatment was able to reduce intestinal damage, body weight loss, and serum BA and largely normalize both the intestinal expression and serum levels of key inflammatory cytokines (Fig. 2F–K and SI Appendix, Fig. S7D and E). Moreover, ILC compositional changes similar to those seen in WT mice were

found in the small intestine LP, most notably reduced CCR6<sup>+</sup> and CD4<sup>+</sup> ILC3s (*SI Appendix, Fig. S7 F–H*).

In agreement with a protective role of FXR, a more severe inflammatory phenotype was seen in whole-body FXR knockout (FXRKO) mice challenged with DSS, including increased serum IL17 levels (Fig. 3 *A–D* and *SI Appendix, Fig. S8 A–D*). The percentages of ILCs, and ILC3s in particular, were ~5–7 fold higher in FXRKO mice (Fig. 3*E* and *SI Appendix, Fig. S8E*). This increase in ILC3s was compounded by a ~4-fold increase in functionality, as determined by the proportion of IL17A<sup>+</sup> cells and the increase in expression of signature cytokines (Fig. 3 *E* and *F* and *SI Appendix, Fig. S8E*). In addition, the frequency of pathogenic IL17<sup>+</sup>IFN $\gamma$ <sup>+</sup> Th17 cells was doubled in FXRKO mice (*SI Appendix, Fig. S8D*). Similarly, an exaggerated ADSS phenotype was evident in WT mice transplanted with FXRKO bone marrow, including increased IL17A<sup>+</sup> ILC3s and serum IL17 levels (Fig. 3 *G–J* and *SI Appendix, Fig. S8F*). Furthermore, in an inducible FXR<sup>fllox</sup>/Rorc<sup>cre</sup> model where FXR is selectively reduced in Th17 and ILC3 cells, FexD treatment failed to block DSS-induced changes in cytokine and ILC signature gene expression in LP immune cells, the increases in ILC2s and ILC3s, or the increase in IL17A<sup>+</sup>ILC3s (Fig. 3 *K–P* and *SI Appendix, Fig. S8 G–L*). Given the limited FXR expression in Th17 cells (*SI Appendix, Fig. S6N*), these findings support FXR signaling in ILCs in the regulation of intestinal inflammation. Importantly, the protective effects of FXR agonism were evident in an intervention model, where normalization of serum IL17 and IL6 levels was associated with a reduction in ILC3s in the LP in a chronic DSS model (*SI Appendix, Fig. S9 A–L*).

#### ILC3 Intrinsic FXR Regulates Th17 Function via Cellular Crosstalk.

To provide insights into the cellular crosstalk underlying the in vivo changes in T cells, the ability of ILC-secreted factors to affect Th17 cell differentiation/function was determined. Conditioned media from ILCs, isolated from ADSS-challenged mice and treated ex vivo with FexD or T- $\beta$ MCA, affected the in vitro differentiation of naive CD4<sup>+</sup> T cells, most notably the secretion of IL17 (*SI Appendix, Fig. S10 A–C*). Moreover, the correlation between the opposing effects of the FXR agonist and antagonist on the secretion of IL2 and IL10 from ILCs (34) with the effects of ILC conditioned media on Th17 cell functionality implicated these cytokines as potential mediators of in vivo cellular crosstalk (33) (*SI Appendix, Fig. S10 A–D*).

#### FXR Regulates ILC3 Development and Functional Maturation.

The ILC compositional changes seen in FexD-treated IBD models implicated FXR as an intrinsic regulator of ILC development and functional maturation. To explore this effect, single-cell transcriptomic analyses (scRNA-seq) were performed on ILCs isolated from ADSS mice. The expression of signature genes revealed 9 discrete cell clusters, including 2 ILC2 and 2 ILC3 clusters (Fig. 4*A* and *SI Appendix, Figs. S11–S13* and Table S1) (7, 16, 30, 35). In addition, a small proportion of precursor-like (preILC-like) cells was evident (Fig. 4*A*), consistent with the recruitment of circulating preILCs upon an inflammatory stimulus (6, 35–37). Treatment with FexD reduced the relative proportions of the ILC subsets including a 3-fold reduction in ILC3s and lowered the expression of *Il17f* and *Il22* in the ILC3 clusters (Fig. 4 *B* and *C* and *SI Appendix, Figs. S14–S16* and Table S2). These population changes were accompanied by decreased expression of signature cytokines, transcription factors, and metabolic genes, as well as commitment markers (Fig. 4*D* and *SI Appendix, Figs. S17A* and *S18 A–D*). Moreover, a preILC-like population, expressing higher levels of the precursor marker *Tox*, was increased more than 10 fold in treated mice, consistent with a role for FXR in the

functional maturation of ILCs (Fig. 4 *B* and *D* and *SI Appendix, Figs. S17D* and *S18D*) (6, 13, 36–39).

To support FXR as a determining factor in the functional maturation of intestinal ILCs, a differentiation trajectory was constructed from the single-cell transcriptional data using precursor (*Tox* and *Tox2*) and differentiated cell signature genes (e.g., *Tcf7*, *Gjb2*, *Batf3*, *Rorc*, and *Nr1d1* in ILC3s) (37, 39–42) (*SI Appendix, Fig. S18 E–I*). The resultant lineage trajectory confirmed the pre-ILC-like cluster as a precursor population with multilineage potential (6) (Fig. 4*E*). In addition, the projection of RNA velocities (calculated based on the ratio of unspliced to spliced mRNA) onto the tSNE map revealed altered developmental trajectories in FexD-treated cells (40) (*SI Appendix, Fig. S17 B* and *C*). Moreover, these *in silico* analyses were consistent with the changes in marker gene expression in LP immune cells and the increase in PLZF<sup>+</sup> and ID2<sup>+</sup> preILCs in FexD-treated mice (6, 9, 36, 43–45) (Fig. 4 *F* and *G* and *SI Appendix, Fig. S17 E* and *F*). Of note, FexD inhibited the in vitro differentiation of PLZF<sup>high</sup> innate lymphoid common precursors (ILCPs) isolated from the bone marrow of PLZF<sup>GFP<sup>cre</sup></sup> mice (GFP<sup>+</sup>CD45.2<sup>+</sup>Lin<sup>−</sup>CD127<sup>+</sup> cells<sup>6</sup>), phenocopying the in vivo effects (Fig. 4 *H–K* and *SI Appendix, Fig. S17 G–I*).

Expression of *Il17* in Th17 and ILC3 cells is transcriptionally regulated by the opposing actions of ROR $\gamma$ t (Rorc, transcriptional activator) and REVERB $\alpha$  (*Nr1d1*, transcriptional repressor) (46), (39, 41, 42). To provide insights into how FexD treatment suppresses *Il17* expression, we initially utilized an *Il17* luciferase reporter (2.0 kb core promoter containing a known ROR $\gamma$ t binding site (47)) to establish a cell-intrinsic effect of FXR (Fig. 4*L*). Of note, the REVERB $\alpha$  agonist SR9009 used as a positive control in these studies has been reported to have effects independent of REVERB $\alpha$ . Given the induction of *Nr1d1* by FexD in ADSS mice and ex vivo treated ILC3s (Figs. 2*D* and 4*G*), and the presence of FXR binding sites in both the gene body and regulatory regions of *Nr1d1* in mouse liver and intestinal tissues (48) (*SI Appendix, Fig. S17J*), we posited that REVERB $\alpha$  is a downstream effector of FXR in ILCs. In support of this notion, FXR induced dose- and ligand-dependent activation of a luciferase reporter under the control of the REVERB $\alpha$  promoter in HEK293T cells cotransfected with human or mouse FXR, while having no effect in comparable experiments with the RORc promoter (Fig. 4*M* and *SI Appendix, Fig. S17 K–M*).

In combination, the above findings support a key role for FXR signaling in the differentiation and functional maturation of intestinal ILCs in response to an inflammatory challenge and, combined with the secondary effects on T cell responses, point to the potential of FXR as a therapeutic target in intestinal inflammatory diseases such as IBD (6, 31, 36, 49, 50).

## Discussion

As early dietary sensors and genetic effectors, BA have emerged as pleiotropic signaling molecules important in gut epithelial regeneration and mucosal immunity (25–27, 51). Notably, bile acid levels are increased in IBD, in concert with decreased FXR signaling in the ileum of Crohn's disease patients (28). Reciprocally, FXR agonists reduce intestinal inflammation and epithelial permeability (20, 25, 52). Here, we show in an aggressive DSS-induced inflammation model that attenuation of the innate immune cell response contributes to the protective effects of FXR activation.

Tissue-specific ILC subtypes develop from circulating precursor cells in response to local environmental cues (10, 11, 50, 53). In the gut, ILCs function as early effectors, secreting cytokines that activate and regulate both the innate and adaptive immune

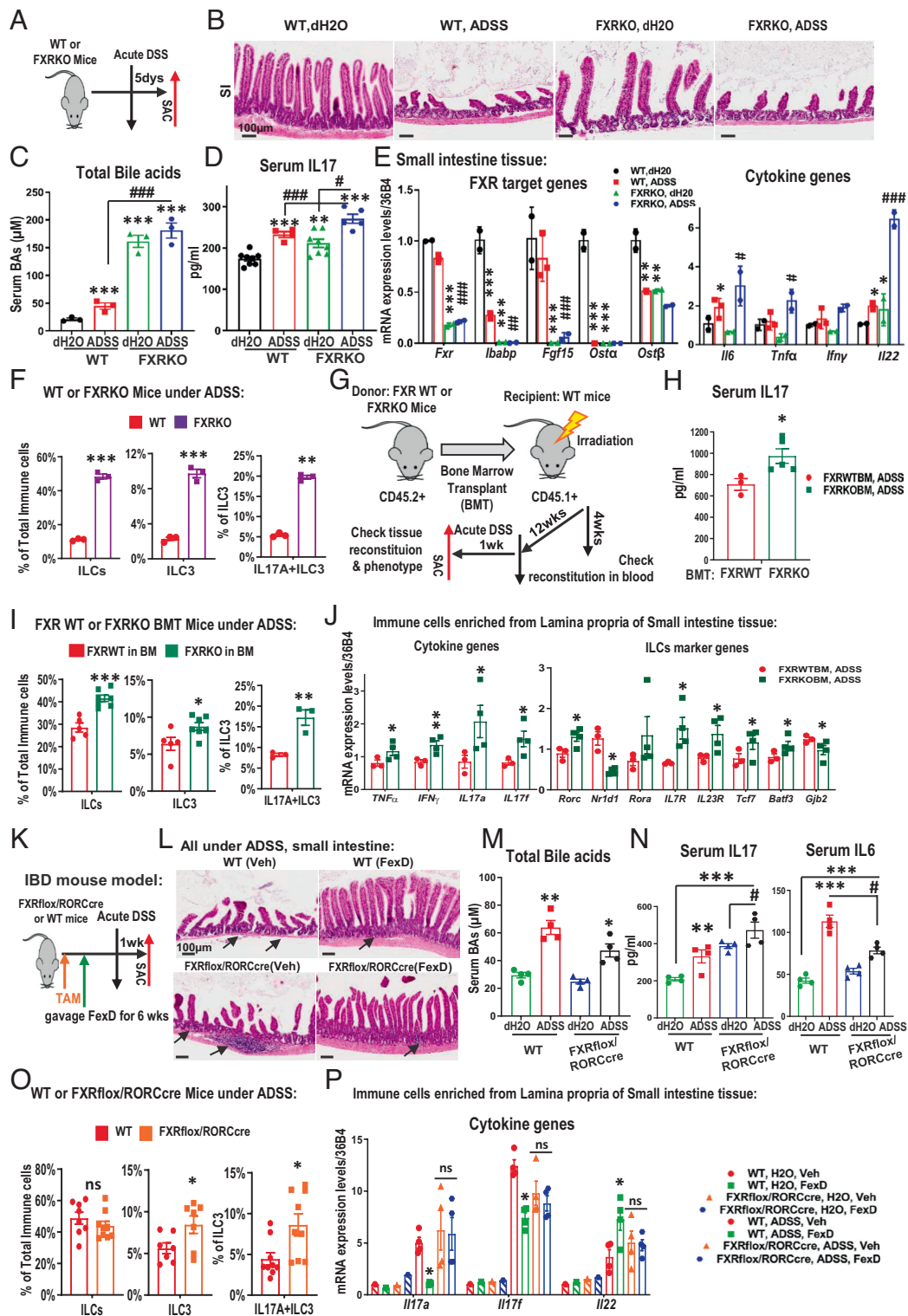


**Fig. 3.** FXR attenuates intestinal ILC3 responses to inflammatory insults. (A) Experimental scheme of WT and whole-body FXRKO mice subjected to ADSS administration, for panels B–F. (B) Representative H&E staining of small intestine (Scale bar, 100 μm.) (C and D) Serum bile acid (C, n = 3 per arm) and IL17 levels (D, n = 8 H<sub>2</sub>O-treated WT and FXRKO; n = 4 and 5 DSS-treated WT and FXRKO mice). (E) Expression of FXR target and cytokine genes in small intestine tissue, measured by qRT-PCR (n = 3 to 5). (F) ILC and ILC3 (percentages of total immune cells) and IL17A<sup>+</sup> ILC3 (percentage of ILC3s) cell numbers in ADSS-treated WT and FXRKO mice (n = 3 per arm). (G) Scheme of bone marrow transplants (BMT) from WT and FXRKO donor mice prior to ADSS challenge, for panels I–K. (H) Serum IL17 levels (n = 3 FXRWT, n = 5 FXRKO). (I) ILC and ILC3 (percentages of total immune cells) and IL17A<sup>+</sup> ILC3 (percentage of ILC3s) cell numbers in mice receiving WT and FXRKO BMTs (n = 5 and 7, respectively). (J) Expression of cytokine and ILC lineage commitment marker genes in small intestine tissue, measured by qRT-PCR. (K) Experimental scheme of WT and FXR conditional knockout (RORC<sup>+</sup> cells) mice challenged by ADSS, for panels M–Q. (L) Representative H&E staining of small intestine. Arrows indicate neutrophil infiltration (Scale bar, 100 μm.) (M and N) Serum bile acid (M, n = 4 per arm), and IL17 and IL6 levels (N, n = 4 per arm). (O) Total ILC, ILC3, and IL17A<sup>+</sup> ILC3 cell numbers in small intestine lamina propria (n = 8 per arm). (P) Expression of cytokine genes in immune cells isolated from the LP of the small intestine, measured by quantitative RT-PCR (n = 4 per arm). Experiments were independently replicated 2 to 6 times, with representative data shown as the mean ± SEM. \* ADSS versus vehicle; # FexD versus vehicle; \* # P < 0.05; \*\* P < 0.01; \*\*\* P < 0.005. Student's unpaired t test was used for two-way comparisons; one-way ANOVA test followed by multiple comparisons was used to compare multiple groups.



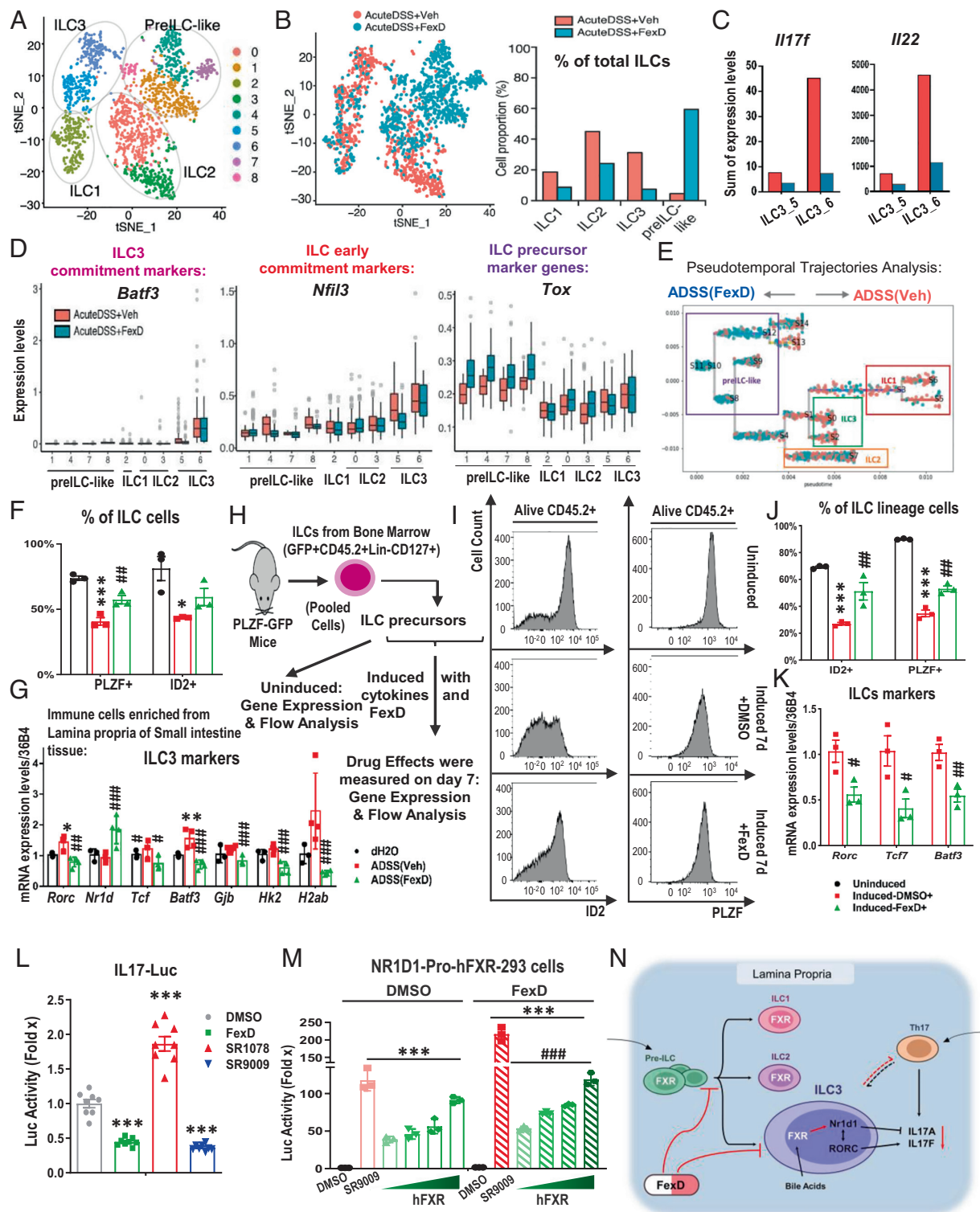


**Fig. 4.** FXR regulates ILC3 development and functional maturation. (A and B) tSNE plots of ILC clusters (A) and FexD-induced changes (B) identified from single-cell RNA sequencing (n = 4 pooled). (C) ILC subtype composition (Left) and cumulative *I17f* and *I122* expression in ILC3 clusters (Right). (D) Box plots of ILC commitment markers *Batf3*, *Nfil3*, and *Tox* expression. (E) Pseudotemporal trajectories of ILCs based on scRNA-seq data. (F) PLZF<sup>+</sup> and ID2<sup>+</sup> ILC progenitor cells in the LP of WT mice, treated as indicated in G. (G) Expression of ILC3 commitment markers in immune cells enriched from small intestine LP of indicated models (measured by RT-qPCR: n = 3, control; n = 4 ADSS ± FexD). (H) Experimental scheme for in vitro differentiation of ILCs, for panels I–K. (I) Histograms of ID2<sup>+</sup> and PLZF<sup>+</sup> cell numbers before and 7 d after differentiation with and without FexD treatment. (J) ID2<sup>+</sup> and PLZF<sup>+</sup> cell numbers, expressed as percentage of ILC lineage cells, measured by flow cytometry. (K) Expression of signature ILC marker genes measured by RT-qPCR (n = 3, per arm). (L) Effects of FXR agonist (FexD), RORγt agonist (SR1078), and REVERBα agonist (SR9009) on *IL17* expression, as measured by luciferase reporter activity in HEK293T cells (2.0 kb core promoter). (M) Effects of increasing levels of human FXR on *Nr1d1* expression with and without FexD treatment, as measured by luciferase reporter activity in HEK293T cells, with DMSO as negative control and *Nr1d1* agonist (SR9009) as positive control. (N) Schematic model depicting the beneficial effects of FXR activation in intestinal immune cells. Experiments were independently replicated three times, with representative data shown as the mean ± SEM; \* and #, *P* < 0.05; \*\* and ##, *P* < 0.01; and \*\*\* and ###, *P* < 0.005. Student's unpaired *t* test was used for two-way comparisons; one-way ANOVA test followed by multiple comparisons was used to compare multiple groups.

responses (32, 53). In particular, ILC3s respond to extracellular bacteria and maintain tolerance to intestinal commensals (4, 49, 54). While an increase in T<sub>eff</sub> cells is a hallmark of IBD (17), we show that FexD reduces inflammatory cytokines by directly affecting the differentiation and functional maturation of ILCs (36, 37). Indeed, FexD fails to affect naive T cells, in agreement with the negligible levels of FXR expression. In contrast, our single-cell analyses of ILCs from the inflamed gut indicated that activation of FXR not only sharply reduced total ILC numbers but also decreased the signature transcriptional factors (including *Tcf7*, *Batf3*, *Rora*, and *Gata3*) and functional cytokines (most notably, IL17F and IL22, Fig. 4 and *SI Appendix, Fig. S18*), particularly in ILC3 and ILC2 (30). Strikingly, FexD increased the population of preILC-like cells (Fig. 4B). In accordance, FexD coordinately upregulated the expression of key transcriptional factors associated with early ILC progenitors (ILCP; including *Id2*, *Tox*, and *Tox2*) while downregulating ILC early commitment transcriptional factors (*Nfil3* and *IL2ra*) (Fig. 4 and *SI Appendix, Figs. S17 and S18*) (6, 36, 37, 50). Our findings suggest that FXR signaling regulates the commitment of ILC precursors into functional ILCs and implicates the transcriptional repressor REVERB $\alpha$  as a downstream effector of FXR (Fig. 4N and *SI Appendix, Fig. S17*). While the functional impact of an increased precursor population is currently unknown, the influx of preILC-like cells is expected to significantly decrease in the absence of an inflammatory insult. Recently, the clinical effects of FXR agonists such as obeticholic acid (55) have been explored extensively in liver steatosis and cirrhosis (29, 56). By extension, pharmacologic FXR activation may offer a new integrative strategy offering synergistic effects in both intestinal epithelial cells and innate immune cells.

**Data, Materials, and Software Availability.** The accession number for the single-cell RNA-seq data reported in this paper is NCBI SRA: [PRJNA557472](https://www.ncbi.nlm.nih.gov/sra/PRJNA557472).

**ACKNOWLEDGEMENTS.** We thank Y.Z. for providing the Rorc-GFP mice; Y. Liang, Q. Yang, Y. Dai, W. Waizenegger, H. Juguilon, and L. Chong for technical assistance; C. O'Connor and C. Fitzpatrick in Salk FACS core; C. Fine and J. Olvera in UCSD FACS core; N. Hah and G. Chou in Salk NGS Core; Y. Zhu for scientific and technical suggestions; D. O'Keefe for editorial assistance; and L. Ong and C. Brondos for administrative assistance. This work was funded by grants from the NIH (DK057978, HL105278, and HL088093), National Cancer Institute (CA014195), National Health and Medical Research Council of Australia Project grants (grant 1087297 to C.L. and M.D.), the Leona M. and Harry B. Helmsley Charitable Trust (2017PG-MED001), and an SWCRF Investigator Award. T.F. is supported by Hewitt Medical Foundation Fellowship, a Salk Alumni Fellowship, and Crohn's & Colitis Foundation (CCFA) Visiting IBD Research Fellowship. M.D. and R.M.E. are supported, in part, by a Stand Up To Cancer-Cancer Research UK-Lustgarten Foundation Pancreatic Cancer Dream Team Research Grant (Grant Number: SU2C-AACR-DT-20-16). Stand Up To Cancer is a program of the Entertainment Industry Foundation. Research grants are administered by the American Association for Cancer Research, the scientific partner of SU2C. R.M.E. was supported by the HHMI, March of Dimes Chair in Molecular and Developmental Biology, and NOMIS Foundation Distinguished Scientist and Scholar at the Salk Institute. Research reported in this publication was also supported by the National Institute of Environmental Health Sciences of the National Institutes of Health under Award Number P42ES010337. The content is solely the responsibility of the authors and does not necessarily represent the official views of the National Institutes of Health.

Author affiliations: <sup>a</sup>Gene Expression Laboratory, The Salk Institute for Biological Studies, La Jolla, CA 92037; <sup>b</sup>Storr Liver Centre, Westmead Institute for Medical Research and Sydney Medical School, University of Sydney, Westmead NSW 2145, Australia; and <sup>c</sup>Immunobiology and Microbial Pathogenesis Laboratory, The Salk Institute for Biological Studies, La Jolla, CA 92037

- W. S. Garrett, J. I. Gordon, L. H. Glimcher, Homeostasis and inflammation in the intestine. *Cell* **140**, 859–870 (2010).
- A. Kaser, S. Zeissig, R. S. Blumberg, Inflammatory bowel disease. *Annu. Rev. Immunol.* **28**, 573–621 (2010).
- L. W. Peterson, D. Artis, Intestinal epithelial cells: Regulators of barrier function and immune homeostasis. *Nat. Rev. Immunol.* **14**, 141–153 (2014).
- H. Chu *et al.*, Gene-microbiota interactions contribute to the pathogenesis of inflammatory bowel disease. *Science* **352**, 1116–1120 (2016).
- M. Friedrich, M. Pöhl, F. Powrie, Cytokine networks in the pathophysiology of inflammatory bowel disease. *Immunity* **50**, 992–1006 (2019).
- M. G. Constantinides, B. D. McDonald, P. A. Verhoef, A. Bendelac, A committed precursor to innate lymphoid cells. *Nature* **508**, 397–401 (2014).
- A. K. Björklund *et al.*, The heterogeneity of human CD127(+) innate lymphoid cells revealed by single-cell RNA sequencing. *Nat. Immunol.* **17**, 451–460 (2016).
- G. Eberl, M. Colonna, J. P. Di Santo, A. N. McKenzie, Innate lymphoid cells: A new paradigm in immunology. *Science* **348**, aaa6566 (2015).
- G. Gasteiger, X. Fan, S. Y. Lee, A. Y. Rudensky, Tissue residency of innate lymphoid cells in lymphoid and nonlymphoid organs. *Science* **350**, 981–985 (2015).
- E. Kugelberg, Innate lymphoid cells: Nutrients direct immune balance. *Nat. Rev. Immunol.* **14**, 137 (2014).
- S. P. Spencer *et al.*, Adaptation of innate lymphoid cells to a micronutrient deficiency promotes type 2 barrier immunity. *Science* **343**, 432–437 (2014).
- M. Cella *et al.*, Publisher correction: Subsets of ILC3-ILC1-like cells generate a diversity spectrum of innate lymphoid cells in human mucosal tissues. *Nat. Immunol.* **20**, 1405 (2019).
- J. C. Martin *et al.*, Single-cell analysis of Crohn's disease lesions identifies a pathogenic cellular module associated with resistance to anti-TNF therapy. *Cell* **178**, 1493–1508 e1420 (2019).
- A. Geremia *et al.*, IL-23-responsive innate lymphoid cells are increased in inflammatory bowel disease. *J. Exp. Med.* **208**, 1127–1133 (2011).
- J. H. Bernink *et al.*, Interleukin-12 and -23 control plasticity of CD127(+) group 1 and group 3 innate lymphoid cells in the intestinal Lamina Propria. *Immunity* **43**, 146–160 (2015).
- N. A. Yudanin *et al.*, Spatial and temporal mapping of human innate lymphoid cells reveals elements of tissue specificity. *Immunity* **50**, 505–519 e504 (2019).
- W. Cao *et al.*, The xenobiotic transporter Mdr1 enforces T cell homeostasis in the presence of intestinal bile acids. *Immunity* **47**, 1182–1196 e1110 (2017).
- H. Wang, J. Chen, K. Hollister, L. C. Sowers, B. M. Forman, Endogenous bile acids are ligands for the nuclear receptor FXR/BAR. *Mol. Cell* **3**, 543–553 (1999).
- M. Downes *et al.*, A chemical, genetic, and structural analysis of the nuclear bile acid receptor FXR. *Mol. Cell* **11**, 1079–1092 (2003).
- S. Fang *et al.*, Intestinal FXR agonism promotes adipose tissue browning and reduces obesity and insulin resistance. *Nat. Med.* **21**, 159–165 (2015).
- J. T. Gaublot *et al.*, Single-cell genomics unveils critical regulators of Th17 cell pathogenicity. *Cell* **163**, 1400–1412 (2015).
- C. Wang *et al.*, CD5LAIM regulates lipid biosynthesis and restrains Th17 cell pathogenicity. *Cell* **163**, 1413–1427 (2015).
- J. H. Bernink *et al.*, c-Kit-positive ILC2s exhibit an ILC3-like signature that may contribute to IL-17-mediated pathologies. *Nat. Immunol.* **20**, 992–1003 (2019).
- C. Tang *et al.*, Suppression of IL-17F, but not of IL-17A, provides protection against colitis by inducing Treg cells through modification of the intestinal microbiota. *Nat. Immunol.* **19**, 755–765 (2018).
- T. Fu *et al.*, FXR regulates intestinal cancer stem cell proliferation. *Cell* **176**, 1098–1112 e1018 (2019).
- R. Chevre, C. Silvestre-Roig, O. Soehnlein, Nutritional modulation of innate immunity: The fat-bile-gut connection. *Trends Endocrinol. Metab.* **29**, 686–698 (2018).
- P. Vavassori, A. Mencarelli, B. Renga, E. Distrutti, S. Fiorucci, The bile acid receptor FXR is a modulator of intestinal innate immunity. *J. Immunol.* **183**, 6251–6261 (2009).
- R. M. Nijmeijer *et al.*, Farnesoid X receptor (FXR) activation and FXR genetic variation in inflammatory bowel disease. *PLoS One* **6**, e23745 (2011).
- R. M. Gadaleta *et al.*, Farnesoid X receptor activation inhibits inflammation and preserves the intestinal barrier in inflammatory bowel disease. *Gut* **60**, 463–472 (2011).
- M. Gurj-Ben Ari *et al.*, The spectrum and regulatory landscape of intestinal innate lymphoid cells are shaped by the microbiome. *Cell* **166**, 1231–1246 e1213 (2016).
- N. von Burg *et al.*, Activated group 3 innate lymphoid cells promote T-cell-mediated immune responses. *Proc. Natl. Acad. Sci. U.S.A.* **111**, 12835–12840 (2014).
- K. Mao *et al.*, Innate and adaptive lymphocytes sequentially shape the gut microbiota and lipid metabolism. *Nature* **554**, 255–259 (2018).
- L. Zhou *et al.*, Innate lymphoid cells support regulatory T cells in the intestine through interleukin-2. *Nature* **568**, 405–409 (2019).
- S. Bonne-Annee, M. C. Bush, T. B. Nutman, Differential modulation of human innate lymphoid cell (ILC) subsets by IL-10 and TGF- $\beta$ . *Sci. Rep.* **9**, 14305 (2019).
- M. L. Robinette *et al.*, Transcriptional programs define molecular characteristics of innate lymphoid cell classes and subsets. *Nat. Immunol.* **16**, 306–317 (2015).
- W. Xu *et al.*, An Id2(RFP)-reporter mouse redefines innate lymphoid cell precursor potentials. *Immunity* **50**, 1054–1068 e1053 (2019).
- M. Pokrovskii *et al.*, Characterization of transcriptional regulatory networks that promote and restrict identities and functions of intestinal innate lymphoid cells. *Immunity* **51**, 185–197 e186 (2019).
- C. R. Seehus *et al.*, The development of innate lymphoid cells requires TOX-dependent generation of a common innate lymphoid cell progenitor. *Nat. Immunol.* **16**, 599–608 (2015).
- C. Godinho-Silva *et al.*, Light-entrained and brain-tuned circadian circuits regulate ILC3s and gut homeostasis. *Nature* **574**, 254–258 (2019).
- B. Wang *et al.*, Phospholipid remodeling and cholesterol availability regulate intestinal stemness and tumorigenesis. *Cell Stem Cell* **22**, 206–220 e204 (2018).
- F. Teng *et al.*, A circadian clock is essential for homeostasis of group 3 innate lymphoid cells in the gut. *Sci. Immunol.* **4**, eaax1215 (2019).
- Q. Wang *et al.*, Circadian rhythm-dependent and circadian rhythm-independent impacts of the molecular clock on type 3 innate lymphoid cells. *Sci. Immunol.* **4**, 1215 (2019).



43. C. S. N. Klose *et al.*, Differentiation of type 1 ILCs from a common progenitor to all helper-like innate lymphoid cell lineages. *Cell* **157**, 340–356 (2014).
44. J. K. Bando, H. E. Liang, R. M. Locksley, Identification and distribution of developing innate lymphoid cells in the fetal mouse intestine. *Nat. Immunol.* **16**, 153–160 (2015).
45. A. P. Mao, I. E. Ishizuka, D. N. Kasal, M. Mandal, A. Bendelac, A shared Runx1-bound Zbtb16 enhancer directs innate and innate-like lymphoid lineage development. *Nat. Commun.* **8**, 863 (2017).
46. X. Yu *et al.*, TH17 cell differentiation is regulated by the circadian clock. *Science* **342**, 727–730 (2013).
47. F. Zhang, G. Meng, W. Strober, Interactions among the transcription factors Runx1, RORgammat and Foxp3 regulate the differentiation of interleukin 17-producing T cells. *Nat. Immunol.* **9**, 1297–1306 (2008).
48. A. M. Thomas *et al.*, Genome-wide tissue-specific farnesoid X receptor binding in mouse liver and intestine. *Hepatology* **51**, 1410–1419 (2010).
49. M. R. Hepworth *et al.*, Immune tolerance. Group 3 innate lymphoid cells mediate intestinal selection of commensal bacteria-specific CD4(+) T cells. *Science* **348**, 1031–1035 (2015).
50. A. I. Lim *et al.*, Systemic human ILC precursors provide a substrate for tissue ILC differentiation. *Cell* **168**, 1086–1100 e1010 (2017).
51. C. Ma *et al.*, Gut microbiome-mediated bile acid metabolism regulates liver cancer via NKT cells. *Science* **360**, 5931 (2018).
52. M. Stojancevic, K. Stankov, M. Mikov, The impact of farnesoid X receptor activation on intestinal permeability in inflammatory bowel disease. *Can. J. Gastroenterol.* **26**, 631–637 (2012).
53. O. I. Koues *et al.*, Distinct gene regulatory pathways for human innate versus adaptive lymphoid cells. *Cell* **165**, 1134–1146 (2016).
54. G. Y. Seo *et al.*, LIGHT-HVEM signaling in innate lymphoid cell subsets protects against enteric bacterial infection. *Cell Host Microbe* **24**, 249–260 e244 (2018).
55. C. W. Cheng *et al.*, Ketone body signaling mediates intestinal stem cell homeostasis and adaptation to diet. *Cell* **178**, 1115–1131.e1115 (2019).
56. S. Mudaliar *et al.*, Efficacy and safety of the farnesoid X receptor agonist obeticholic acid in patients with type 2 diabetes and nonalcoholic fatty liver disease. *Gastroenterology* **145**, 574–582.e571 (2013).